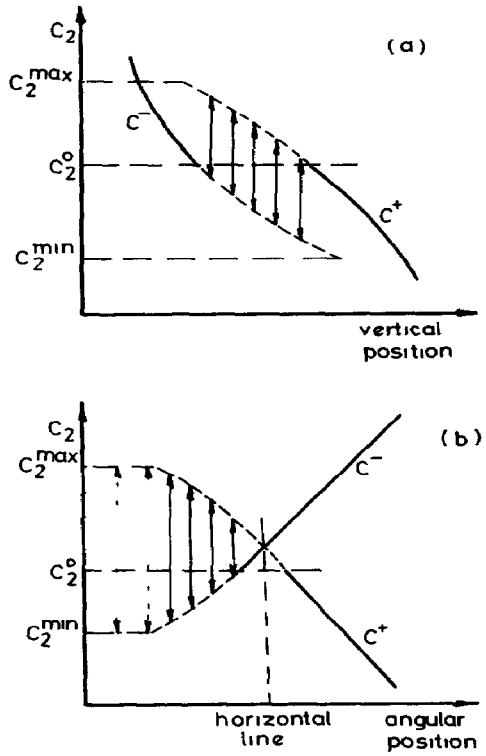

Fig 2 Dependence of the slow variable on the position of the line $r_2 = 0$ (a), downward movement of the line, (b), rotation of the line, —, stable states, ——, metastable states, ↕ relaxation oscillations, ↕ chaotic oscillations

state (which looks like the curves in Fig 1, with c_1 standing for volume and c_2, for pressure) and a horizontal line c_2 = const (see Fig 1c) Two states stable to infinitesimal perturbations exist at pressures between the maximum and the minimum of the S-shaped curve However, below a certain pressure which corresponds to the neutrally stable Maxwell construction, the gaseous state on the right-hand branch is destabilized by growing of liquid nuclei formed due to local perturbations

Above the same pressure, expanding gaseous nuclei destabilize the liquid state on the left-hand branch Alternative states can be realized at the same pressure level only when special precautions against random nucleation help preserving the metastable superheated liquid or supercooled gas

The same picture would be observed in transitions between alternative steady states of a non-equilibrious system with a horizontal null-rate line $r_2 = 0$ Tilting it anticlockwise to the position in Fig 1(a) creates a situation when *both* alternative steady states are metastable On the contrary, when the null-rate line is tilted clockwise to the position in Fig 1(d) so that $c_2^- > c_2^+$ and $I(c_2^-) < 0$, $I(c_2^+) > 0$, the nuclei do not grow, and both steady states are stable That is the only case when hysteresis can be observed in the presence of short-wave perturbations

Figure 2(a) shows how c_2 changes when the line $r_2 = 0$ inclined as in Fig 1(a) is shifted downwards When an intersection with the right-hand branch of the S-shaped curve $r_1 = 0$ first appears, it is metastable Further down, as the intersection on the left hand passes the level $c_2 = c_2^0$, where $I(c_2^0) = 0$, it becomes metastable as well, and chaotic oscillations arise The chaos terminates after the intersection in the right passes the level c_2^0 and thus stabilizes

Figure 2(b) represents evolution of the system caused by rotating the line $r_2 = 0$ clockwise from the position in Fig 1(b) Intersections with the "stable" branches of the S-shaped curve first appear as metastable states The relaxation oscillations, instead of abruptly disappearing, become chaotic, and their amplitude gradually decreases as the line $r_2 = 0$ comes nearer to the horizontal position At the same time, increases the wave length of perturbations needed to nucleate an alternative state (in the same manner as crystals become larger at lower supersaturation) After one of the intersections passes the level c_2^0 with $I(c_2^0) = 0$, the corresponding state stabilizes and oscillations die away Anticlockwise from the horizontal position, the second intersection passes the level c_2^0, and the system becomes multistable This picture demonstrates that a chaotic state appears as a natural transition from ordered relaxation oscillations to multistability

Department of Chemical Engineering L M PISMEN
Technion-Israel Institute of Technology
Haifa, Israel

REFERENCES

[1] Ortoleva P and Ross J , *J Chem Phys* 1975 **63** 3398
[2] Fife P , *J Chem Phys* 1976 **44** 554
[3] Winfree A T , *Proc 9th Symp Far Soc* 1975
[4] Fife P , *AMS-SIAM Symp Asymptotic Methods and Singular Perturbations*, New York 1976

Chemical Engineering Science Vol 34 pp 131–133

0009-2509/79/0101-0131/$02 00/0

An evaluation of radial solid spread factors in a gas–solid packed column at trickle flow

(*Received* 24 *May* 1978, *accepted* 25 *July* 1978)

The trickle flow of a freely flowing solid through a packed column is a promising new gas–solid counter-current operation with possible applications in chemical industry[1, 2] (e g in the continuous adsorption of gases or in chemical reactions, especially equilibrium reactions)

In previous papers[3–5] a gas solid trickle flow column was shown to behave as an almost ideal gas solid counter-current contactor (e g low pressure drop, little axial mixing and a high interphase mass transfer rate)

In the foregoing examinations the gas and solid phases were assumed to be well distributed over the column diameter Consequently the model parameters were considered to be independent of the radial position in the column If, however, the local mass flux of one of the phases diverges strongly from its mean value over the cross section of the column the local capacity ratio of the phases might deviate strongly from unity thus possibly causing local equilibria between the phases This may have a pronounced effect on column performance[6]

In a gas solid trickle flow column the solid phase is introduced through one or more feed points The particles will disperse over the packing while flowing downwards, but dependent on the spreading rate in the upper section of the column the solid phase will be maldistributed If the reflection of the column wall is also known it should be possible to calculate the solid distribution in

any position in the column In this contribution results of the solid mass flux distributions, evaluated from solid spreading experiments the in absence of wall effects, are presented

The radial dissemination of a swarm of particles passing through a packing, in counter-current with a gas, has not been described in open literature before There are, however, two fields which are closely related to this phenomenon viz the spontaneous interparticle percolation as a mechanism for solids (de)mixing and the radial spreading of a liquid through packed column at trickle flow conditions In both fields a diffusional model is frequently used to elucidate the mechanism of radial spreading, e g see [7, 8] We shall use this kind of model also as a first attempt to predict local solid mass flux distributions (possible maldistribution as defined by Groenhof for gas–liquid systems[9], is not taken into account)

The diffusional model for an axisymmetrical point source leads to the following partial differential equation (1)

$$\frac{\partial S}{\partial h} = D\left(\frac{1}{r}\frac{\partial S}{\partial r} + \frac{\partial^2 S}{\partial r^2}\right) \tag{1}$$

In the absence of wall effects the following solution is obtained[10]

$$\frac{S}{S_0} = \frac{1}{4\pi Dh}\exp\left(-\frac{r^2}{4Dh}\right) \tag{2}$$

The solid spread factor D may be obtained from the slope of a plot of $\ln(S/S_0)$ vs r^2 In the present investigation we determined (for the sake of convenience) the solid spread factor from the zeroth moment around the origin of eqn (2)

$$M_0 = \int_{-\infty}^{+\infty} \frac{S}{S_0}\,dr = \frac{1}{\sqrt{(4\pi Dh)}} \tag{3}$$

M_0 can easily be calculated from the experimental data by numerical integration, eqn (3) then allows the evaluation of D

We measured D injecting a freely flowing catalysts carrier (average particle size $70*10^{-6}$ m, other properties are given in [3]) from a point source (internal tube diameter is 0 012 m) on top of the packing and collecting the particles in six coaxial annuli (d = 2 4, 5 2, 8 6, 11 4 and 14 6 10^{-2} m) below the grid plate The annuli were fixed on a porous plate distributor through which air was flowing upwards The column (0 15 m i d) was packed with dumped PALL rings (d_p = 0 015 m), cylindrical screens (d_p = 0 010 m) and RASCHIG rings The diameter of the latter packing material has been varied (5, 10, 15 and 20 10^{-3} m respectively) Details of the experimental set-up have been given elsewhere[11]

Figure 1 gives a typical example of an experimental distribution together wit[redacted] cur[redacted] ccording to eqn (2) Figures 2–4 [redacted] erim[redacted] D for the

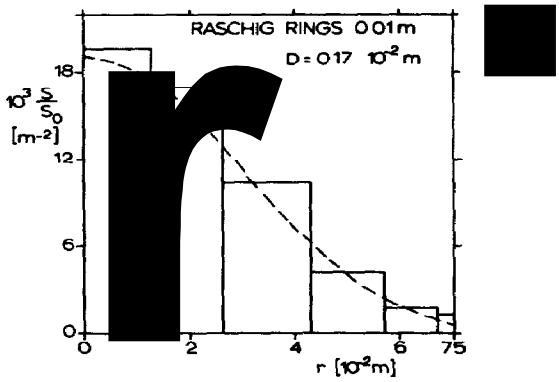

Fig 1 Experimental radial distribution RASCHIG rings (0 010 m) Φ_m = 1 04 kg/m² s, u_g = 0 064 m/s ----, calculated according to eqn (2), D = 0 17 10^{-2} m

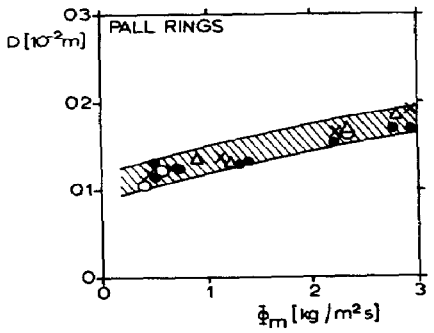

Fig 2 Solid spread factor for PALL rings (0 015 m) vs superficial solid mass flux

Symbol	u_g [m/s]
●	0 064
○	0 093
△	0 12
×	0 16

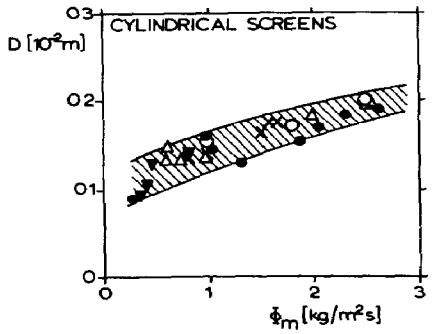

Fig 3 Solid spread factor for cylindrical screens (0 010 m) as a function of solid mass flux (for key to symbols see Fig 2)

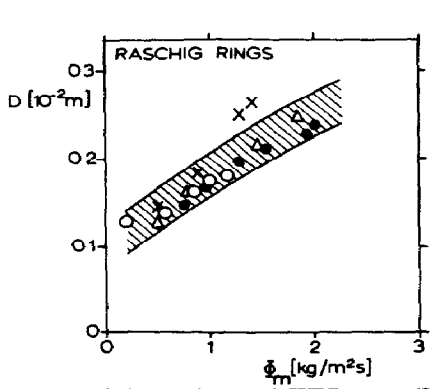

Fig 4 Solid spread factor for RASCHIG rings (0 010 m) vs superficial solid mass flux (for key to symbols see Fig 2)

different packings as a function of the superficial solid mass flux at different gas flow rates In the investigated region the solid spread factor is independent of the superficial gas velocity and increases with an increased solid mass flux In gas–liquid systems the opposite has been observed, the liquid spread factor is independent of the liquid velocity[12] and increases with an increased gas velocity[13]

In gas–liquid systems the packing size was found to have a dominant effect on the liquid spread factor[12, 14, 15] In Fig 5 the radial solid spread factor for RASCHIG rings is plotted vs

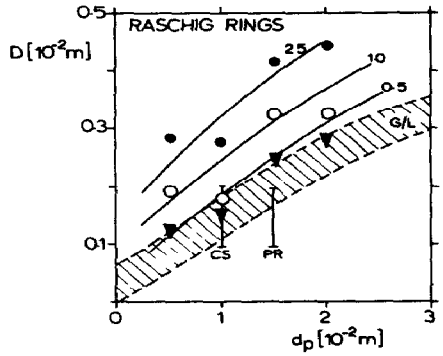

Fig 5 Solid spread factor for RASCHIG rings vs packing diameter

Symbol	Φ_m(kg/m² s)	(CS cylindrical screens PR PALL rings)
▼	0 5	
○	1 0	
●	2 5	

the packing diameter The ranges of the experimental data for PALL rings and cylindrical screens are also given Data for gas liquid systems lie in the shaded area[12, 14, 15] Analogous to the liquid spread factor the solid spread factor increases at enlarged packing sizes At low superficial solid mass fluxes the experimental data for RASCHIG rings almost coincide with the data for gas liquid systems, if the solid mass flux increases the values for the solid spread factor are considerably larger The experimental values for cylindrical screens and PALL rings, however, are much closer to those for gas liquid systems

Acknowledgements—The authors are much indebted to DSM for the financial support (for A W M R) during the course of this work and to F J M Eijsink and H H P Nijkamp who carried out the experiments

†Present address Koninklijke/Shell-Laboratorium, Amsterdam

Department of Chemical Engineering A W M ROES†
Twente University of Technology W P M VAN SWAAIJ
P O Box 217
Enschede, The Netherlands

NOTATION

- D solid spread factor, m
- d_p nominal packing size, m
- h distance between injection point and packing supporting grid, m
- M_0 zeroth moment around the origin of eqn (2), m^{-1}
- r distance from column axis, m
- S local solid mass flux, kg m^{-2} s^{-1}
- S_0 solid mass flow from point source, kg s^{-1}
- u_g superficial gas velocity, m s^{-1}
- Φ_m superficial solid mass flux, kg m^{-2} s^{-1}

REFERENCES

[1] Claus G , Vergnes F and Le Goff P , *Can J Chem Engng* 1976 **54** 143
[2] Van Swaaij W P M , *Proc Int Symp Chem Reac Engng* (Houston 1978), Am Chem Soc Symp Ser part II
[3] Roes A W M and Van Swaaij W P M , *Chem Engng J* , to be published
[4] Roes A W M and Van Swaaij W P M , *Chem Engng J* , to be published
[5] Roes A W M and Van Swaaij W P M , *Chem Engng J* , to be published
[6] Groenhof H C , *Ph D Thesis*, Groningen 1972
[7] Bridgewater J , Sharpe N W and Stocker D C , *Trans Instn Chem Engrs* 1969 **47** T114
[8] Cihla Z and Schmidt O , *Coll Czech Chem Comm* 1957 **22** 896
[9] Groenhof H C , *Chem Engng J* 1977 **14** 193
[10] Carslaw H S and Jaeger J C , *Conduction of Heat in Solids* 2nd Edn, p 50 Oxford at the Clarendon Press, London 1959
[11] Roes A W M , Ph D Thesis, Enschede 1978
[12] Bemer G G and Zuiderweg F J , *Chem Engng Sci* 1978 **33** 1637
[13] Dutkai E and Ruckenstein E , *Chem Engng Sci* 1970 **25** 483
[14] Brignole E A , Zacharonek G and Magnosio J , *Chem Engng Sci* 1973 **28** 1225
[15] Onda K , Takeuchi H , Maeda Y and Takeuchi N , *Chem Engng Sci* 1973 **27** 1677

Chemical Engineering Science Vol 34 pp 133–135

0009–2509/79/0101–0133/$02 00/0

Design of a pulse diffusivity apparatus for improved sensitivity

(*Received* 7 *April* 1978)

Several techniques have been proposed in the literature to measure effective diffusivities in porous catalysts The counterdiffusion cell technique[1], which applies basic diffusion theory, is a steady-state, single pellet measurement This technique was used in our laboratory for measuring diffusivities for a variety of catalyst supports[2] However, single pellet techniques pose sampling problems if a non-uniform collection of pellets is to be characterized

The pulse (or chromatographic) technique examines the eluted concentration pulse from a packed column after a plug of tracer is injected into the carrier gas stream Waldram[3] reviewed diffusivity measuring techniques and concluded that pulse techniques often failed to provide a sensitive measure of the effective diffusivity because the overall dispersion in a packed bed was only a weak function of the intraparticle diffusivity Scott *et al* [4] observed that the use of a pellet string reactor enables one to reduce axial dispersion effects and thus to enhance the contribution from intrapellet diffusion to the overall pulse dispersion This phenomenon was recently confirmed by Hsiang and Haynes[5] Haynes[6] also theoretically analyzed the effects of carrier gas flow rate and catalyst pellet diameter on the sensitivity of the diffusivity measurement in a bidispersed catalyst support

In practical situations, the catalyst pellet diameter is usually limited to a narrow range Also, the highly sensitive flow-through type detectors which are used for diffusivity studies are often